International RILEM Conference on Materials, Systems and Structures in Civil Engineering
Conference segment on Service life of Cement-Based Materials and Structures
22-24 August 2016, Technical University of Denmark, Lyngby, Denmark

INFLUENCE OF FIBRE REINFORCEMENT ON THE INITIATION OF CORROSION-INDUCED CRACKS

Carlos G. Berrocal [(1)(2)], Ignasi Fernandez [(1)], Karin Lundgren [(1)], Ingemar Löfgren [(1)(2)]

(1) Chalmers University of Technology, Göteborg, Sweden
(2) Thomas Concrete Group AB, Göteborg, Sweden

Abstract

The initiation of corrosion-induced cracks, often running parallel to the reinforcement, becomes a turning point in the service life of a reinforced concrete (RC) structure as they promote increased corrosion rates, thus accelerating the degradation process of the structure. Compared to plain concrete, fibre reinforced concrete (FRC) provides additional confinement to the reinforcement, which has been reported to delay or even prevent the appearance of mechanically induced splitting cracks. In this study, an experimental programme has been carried out to investigate the influence of fibres on the onset of corrosion-induced splitting cracks. Cylindrical lollipop specimens with a centrally positioned Ø16 mm bar and varying cover depths from 40 to 64 mm were subjected to accelerated corrosion. A constant current of 100 $\mu A/cm^2$ was impressed through the specimens and the electrical resistance between each rebar and an external copper mesh acting as cathode was monitored. Crack initiation, determined from a drop in electrical resistance, and confirmed by visual inspection, revealed that fibre reinforcement may delay corrosion-induced cracks, an effect that was more noticeable for reduced *c/Ø ratios*, featuring up to 50% higher corrosion levels at crack initiation compared to plain concrete.

1. Introduction

Corrosion of reinforcement is one of the main causes leading to the premature deterioration of reinforced concrete (RC) structures with the consequent reduction of their service life. In advanced stages of the corrosion process, the accumulation of corrosion products at the steel-concrete interface induces splitting stresses at the concrete cover. If the corrosion does not

cease, the stress level may eventually reach the tensile strength of the concrete and cracking of the cover will occur. Corrosion-induced cracks are typically longitudinal cracks running along the reinforcement. This type of cracks have been reported to accelerate the corrosion rate of reinforcement [1] and might result in spalling of the concrete cover. Thus, they are especially harmful for the integrity of the structure and potentially dangerous as concrete pieces can fall off.

Similar to the mechanism of corrosion-induced cracking, the normal bond stresses arising when rebars are subjected to large slips may induce longitudinal cracks along the concrete cover, which are known to severely affect the bond of reinforcement due to the loss of confinement and are often called bond-splitting cracks. Several studies aimed at investigating the influence of fibres on bond of reinforcement in RC tie-elements, see e.g. [2], [3], reported an enhanced control of such splitting cracks when fibre reinforcement was incorporated.

Research focused on the effect of fibre reinforcement on corrosion-induced cracks is sparse. Hybrid fibre reinforced concrete (HyFRC), i.e. concrete incorporating a combination of fibres featuring different sizes and materials, proved to be effective in supressing crack formation in specimens subjected to accelerated corrosion with an impressed current of 1 mA/cm^2 for 48 h [4]. In that study, however, a relatively high fibre dosage (1.5% vol.) was needed to obtain a concrete exhibiting strain hardening. In another study [5], the role of fibres in controlling crack initiation and reducing bond degradation was experimentally investigated for synthetic fibres added at low dosages (0.15 to 0.30 % vol.). Results from that study showed a delay in crack initiation for increasing fibre dosage in terms of the number of exposure cycles needed to observe cracking. However, none of the aforementioned studies determined the actual steel loss needed to cause corrosion-induced cracking.

The present study aimed at understanding how the addition of steel fibre reinforcement at low dosages might influence the onset of splitting cracks induced by accumulation of corrosion products around an embedded rebar. In particular, the actual steel loss necessary to induce cracking was investigated as a function of the cover to bar diameter ratio. The results presented here are part of a larger experimental programme currently ongoing in which the effect of fibre reinforcement on the residual bond capacity of corroded bars will be investigated.

2. Experiments

For the assessment of crack initiation, experiments were conducted including a total of 30 specimens which can be divided into two groups: (i) specimens corroded until crack detection, here referred to as *low corrosion*, which are the main focus of this paper and (ii) specimens corroded beyond cracking, here referred to as *high corrosion*. The nomenclature of the specimens consists of three letters. The first letter indicates the type of concrete, either plain concrete (P) or fibre reinforced concrete (F). When referring to the concrete mixes alone, the abbreviations PC or FRC will be used, respectively, in the following. The remaining two letters indicate the relative size of the specimen, Small (S), Medium (M) or Large (L) and the corrosion level, either Low corrosion (L) or High corrosion (H). Tab. 1 summarizes the details of the experimental programme.

Table 1: Experimental programme. (Number of specimens in brackets)

	Estimated corrosion level and concrete type			
	Low corrosion - cracking		**High corrosion – (7.5%)***	
c/Ø ratio	**PC**	**FRC**	**PC**	**FRC**
2.5	PSL (3)	FSL (3)	PSH (3)	FSH (3)
3.25	PML (3)	FML (3)	-	-
4.0	PLL (3)	FLL (3)	PLH (3)	FLH (3)

*Estimated steel loss based on Faraday's Law

2.1 Specimen geometry and materials

The specimens designed for the present study were cylinders reinforced with a single ∅16 mm ribbed bar at the centre, which stuck out from one of the circular sides, also known as "lollipop" specimens. The cylindrical shape of the specimens and the position of the rebar in the centre were chosen to obtain uniformly distributed corrosion around the rebar and to prevent preferential cracking directions. The cylinders featured a total height of 100 mm while the rebar was partially encased into a PVC tube, thus providing an effective embedment length of 70 mm. Three different concrete cover to bar diameter ratios (*c/∅*) were investigated, namely 2.5, 3.25 and 4, corresponding to cover depths of 40, 52 and 64 mm, respectively. These cover depths comply with the specifications included in current design codes for reinforced concrete structures exposed to a variety of aggressive environments. Fig. 1 presents the specimens geometry.

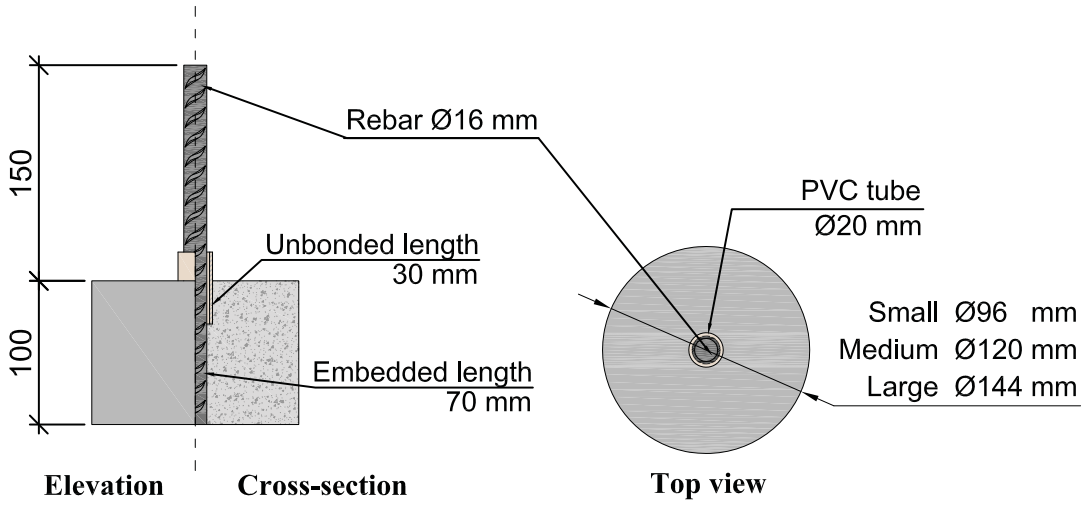

Figure 1: Specimen geometry.

A self-compacting concrete mix with a water to cement ratio (*w/c*) of 0.47 was prepared to cast all the specimens. The same mix composition was used to prepare both the plain and the steel fibre reinforced concrete, except for minor variations in the aggregate content to incorporate the fibres. To promote a fast corrosion initiation, 4% sodium chloride by weight of cement was incorporated into the mix. Tab. 2 shows the detailed concrete composition.

Table 2: Concrete mix proportions, *kg/m³*

	Concrete mix designation	
Component	PC	FRC
Cement (CEM I 42.5N SR 3 MH/LA)	360	360
Limestone filler (Limus 40)	150	150
Fine aggregate (sand 0/4)	718	711
Coarse aggregate (crushed 5/16)	987	977
Effective water	169	169
Superplasticizer – Glenium 51/18	5.4	6.48
Air entrainer – MicroAir 105	0.36	0.36
Sodium Chloride (NaCl)	14.4	14.4
Steel – Dramix 65/35-BN	-	40

The compressive cube strength, f_{cm}, and the splitting tensile strength, f_{ctm}, were assessed for both mixes 28 days after casting through material tests. The former was tested on 100 mm cubes according to [6] while the latter was tested in accordance to [7] on 150 mm cubes. A summary of the material properties is presented in Tab. 3.

Table 3: Compressive and splitting tensile strength, in *MPa*

	f_{cm} **(cube)**		f_{ctm}	
	Avg.	**Std. Dev**	**Avg.**	**Std. Dev**
PC	56.0	1.3	4.2	0.2
FRC	52.5	0.3	4.6	0.2

All the specimens of the same concrete mix were cast in a single batch and were demoulded 24 h after casting. Subsequently, the reference specimens were cured in potable water whereas the remainder, the specimens designated to undergo accelerated corrosion, were cured in 3.5% NaCl solution, all of them at a constant temperature of 22 ºC.

2.2 Experimental setup

Accelerated corrosion tests were carried out in order to hasten the rate of steel dissolution, thus shortening the time necessary to observe corrosion-induced splitting cracks on the concrete cover, which otherwise could take place over a period of months or years. Since detecting the onset of splitting cracks was the main objective of these tests, a specific setup was conceived.

The specimens were introduced into plastic buckets with the reinforcement bar passing through a hole centrally bored at the bottom of the bucket. Silicone was applied at the cylinder surface in order to create a water-tight seal between the specimen and the bucket. A 1 mm thick copper wire mesh, spanning the entire height of the cylinders, was fastened around each specimen using rubber bands. After a 24 h period during which the silicone was left to harden, the buckets were filled with 3.5% NaCl solution, setting the water level about 2 cm below the top of the cylinders. In Fig. 2, the setup of the accelerated corrosion tests is illustrated.

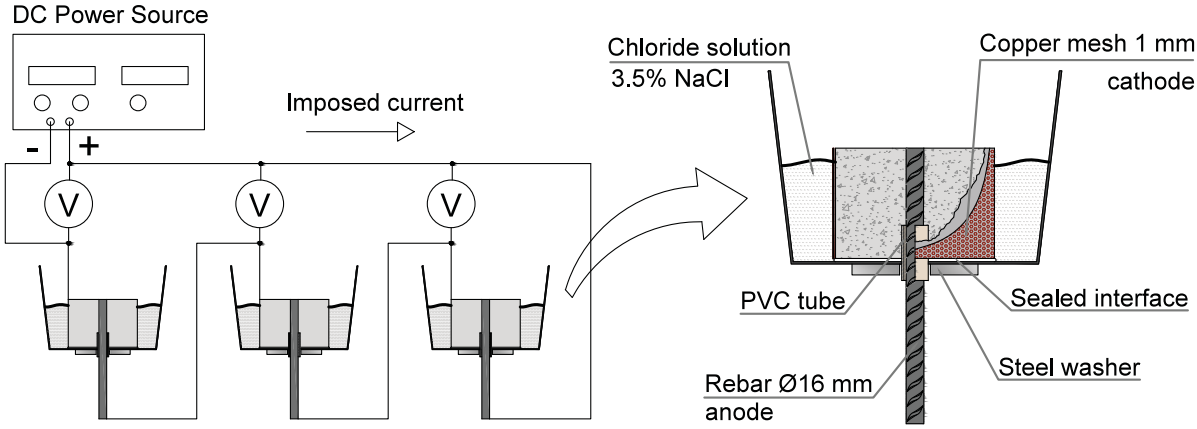

Figure 2: Experimental setup for accelerated corrosion tests

Leads were attached to the reinforcement bar, acting as the anode, and to the copper mesh, acting as the cathode, to connect them to the positive and negative terminals of a power source, respectively. It has been reported in the literature [8] that current densities above 350 $\mu A/cm^2$ may result in deviation of test conditions from a natural corrosion process. Therefore, a steady DC current equal to 3.52 mA was impressed through each specimen which, based on the exposed steel area of embedded rebar, was equivalent to a current density of 100 $\mu A/cm^2$.

The electrical resistance of each specimen was monitored during the entire duration of the accelerated corrosion tests to determine the point in time when corrosion-induced cracking initiated. The potential between each cathode and the positive terminal of the power source was measured and recorded hourly using a data logger. The electrical resistance was calculated, according to Ohm's law, from each individual potential divided by the current intensity passing through the specimen.

In addition to electrical resistance measurements, visual confirmation of the first crack appearance was sought-after. Despite cracks were not easily detectable on the lateral sides of the cylinder due to the copper mesh, the configuration shown in Fig. 2 enabled easy access to the top surface of the specimens on which cracking was likely to be earliest detectable.

Once the accelerated corrosion procedure was completed, the reinforcement bars were extracted and cleaned for gravimetric steel loss measurements. Corrosion products were chemically removed according to ASTM recommendations [9] by repeated immersion of the bars in a solution of hydrochloric acid and urotropine. The corrosion level was calculated for each

reinforcing bar assuming that the measured steel loss was concentrated on the 70 mm bar length embedded in the concrete, according to Eq. 1:

$$v = \frac{M_0 - M_f}{L_e \cdot A_s \cdot \rho} \cdot 100 \quad (1)$$

where v is the corrosion level in %, L_e is the embedded length equal to 70 mm, A_s is the nominal cross-sectional area of the bar equal to 201 mm^2, ρ is the density of steel equal to 7.85 g/cm^3 and M_0 and M_f is the steel weight of the bar before and after the accelerated corrosion, respectively.

3. Results and discussion

Corrosion-induced cracks, which facilitate the transport of ions through concrete, usually result in a sudden drop of the concrete's electrical resistance. Ideally, such phenomenon could be used as a criterion to determine crack initiation. In practice, if cracks are below a certain threshold, the change in transport properties is very limited and the loss of electrical resistance might not be significant.

The electrical resistance of concrete is, furthermore, influenced by numerous factors, e.g. the temperature, the degree of saturation, the chemical composition of the pore solution, etc., while measurements may also be affected by small perturbations in the impressed current. The result is that the development of electrical resistance in time, when observed locally, may continuously fluctuate. Consequently, the specimens in the *low corrosion* series underwent accelerated corrosion until a crack was visually detected, meaning that the corrosion level assessed by gravimetric methods exceeded the actual corrosion level at crack initiation by a certain amount.

In order to determine the corrosion level at crack initiation, electrical resistance results are presented versus the corrosion level based on the steel loss measured at the end of the tests and assuming a linear dependence between time and mass loss. This assumption was based on Faraday's law, provided that a constant corrosion rate was enforced through the impressed current. Fig. 3 presents the variation of the electrical resistance monitored during the time period of the accelerated corrosion procedure for each specimen in the *low corrosion* series. For comparison purposes, in Fig. 4, the variation of the electrical resistance versus corrosion time is presented during the initial 40 days for specimens in the *high corrosion* series, which are still subjected to accelerated corrosion.

As observed, the electrical resistance generally followed a similar pattern in all cases: after an initial drop, it increased and remained rather stable, until it finally decreased again. Crack initiation was determined as the moment when electrical resistance started decreasing with no subsequent significant increase, which is indicated in Fig. 3 and Fig. 4 by arrows. The crack initiation results are summarized in Fig. 5, in which the effect of varying the *c/Ø* ratio and the effect of fibres can be interpreted.

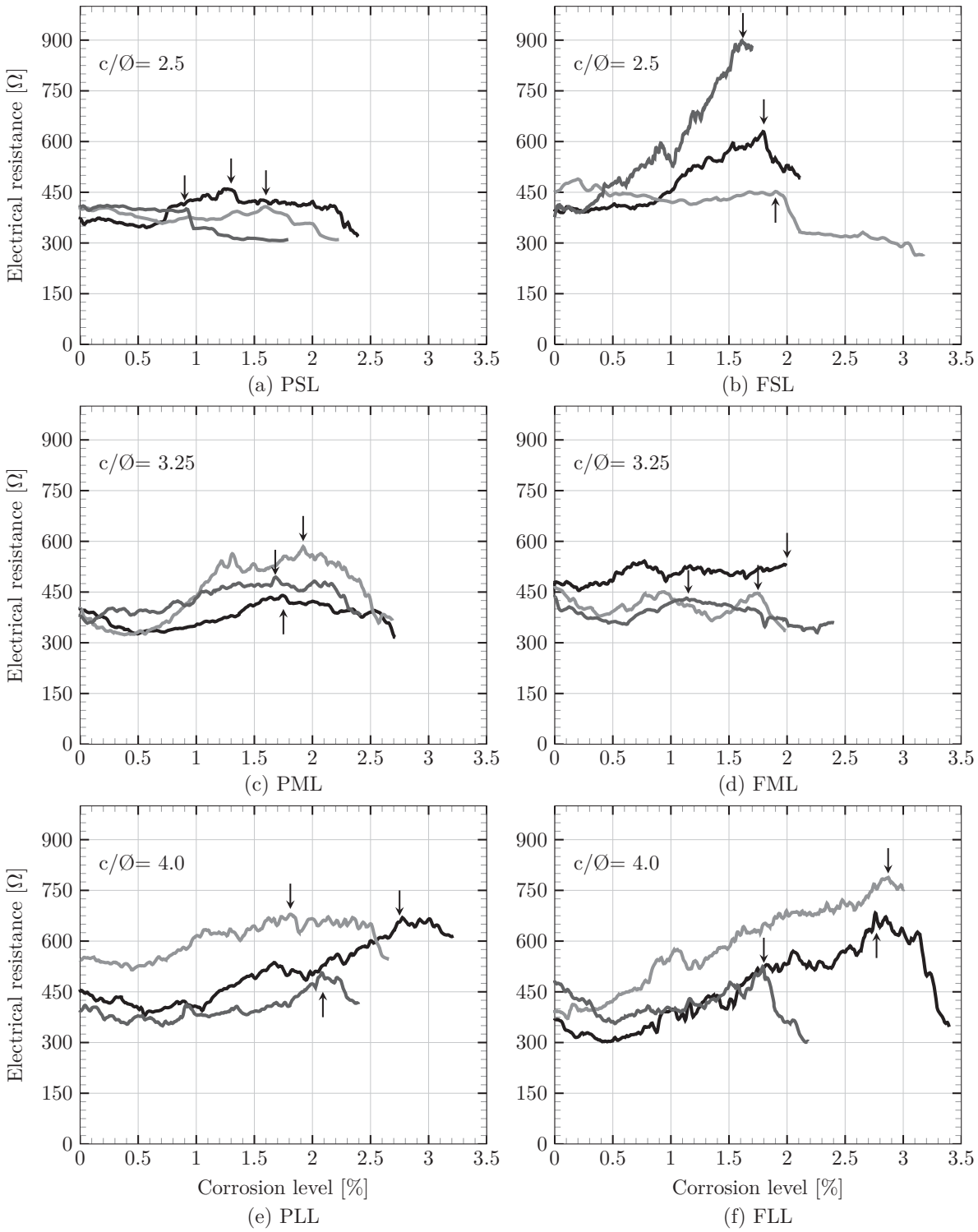

Figure 3: Electrical resistance measurements for *Low corrosion* specimens. Crack initiation is indicated by arrows.

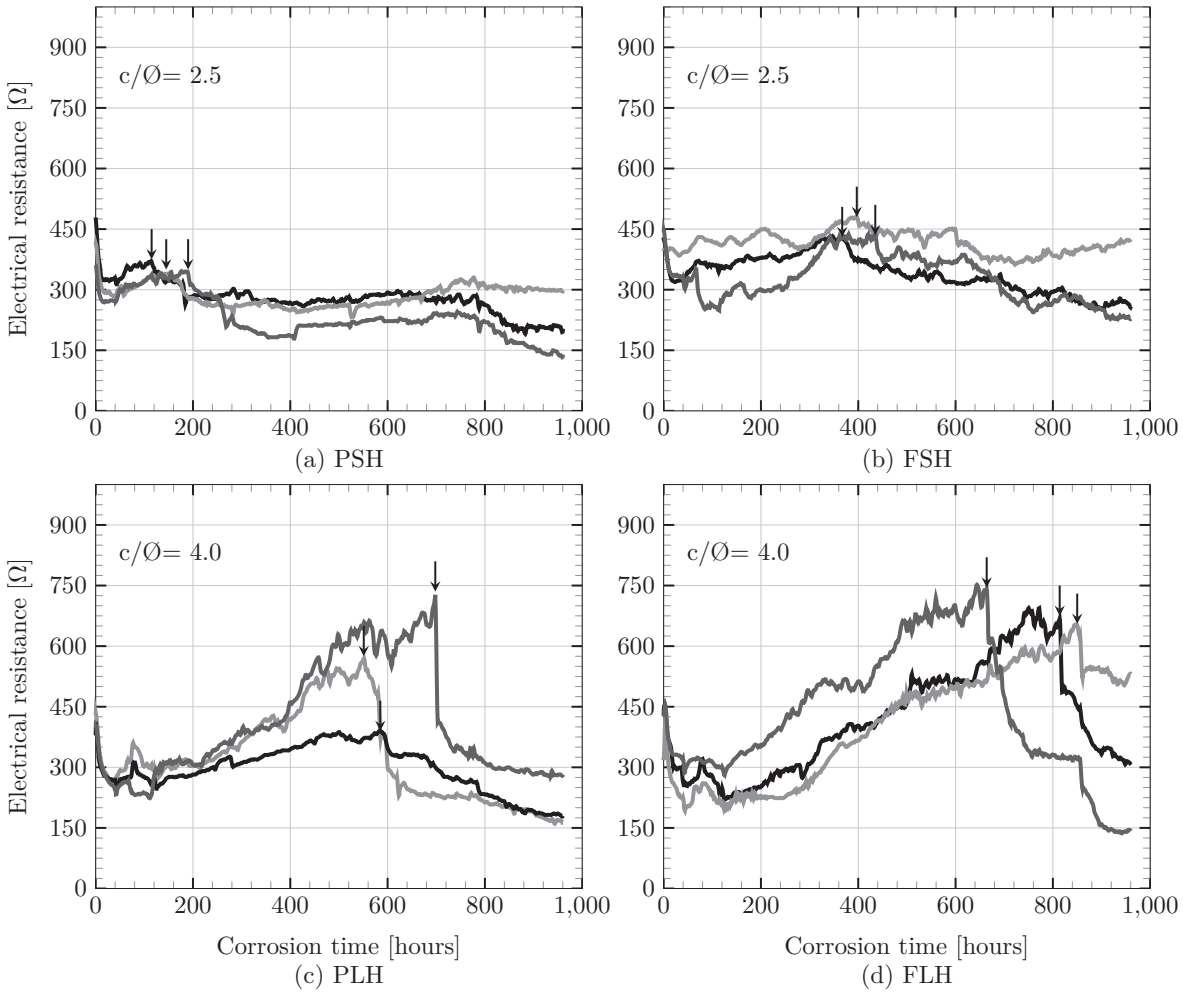

Figure 4: Electrical resistance measurements for *High corrosion* specimens. Crack initiation is indicated by arrows.

It is clear from Fig. 5 that the *c/Ø* ratio played an important role in delaying crack initiation, which based on Fig. 5(a) seemed to keep an almost linear relationship with the corrosion level required to induce cracking. Note that the specimens in the FML group exhibited an unexpectedly low corrosion level, even lower than that of the specimens with smaller dimensions. Consequently, they were considered as outliers but are included here for completeness. The addition of steel fibres at 0.5% vol. also showed a beneficial effect in terms of delayed corrosion-induced cracks although this effect seemed to be dependent on the *c/Ø* ratio. For the smallest specimen size, fibres had a significant impact, which decreased as the *c/Ø* ratio increased. This was likewise observed in Fig. 5(b) for the *high corrosion* series. This size dependent effect was attributed to differences in how cracks propagated in the various size specimens, more gradually in small specimens allowing a greater contribution of the fibres and more suddenly in large specimens due to higher built-up internal pressure. This finding is corroborated by the electrical resistance evolution curves, in Fig. 3 and particularly in Fig. 4, which show a larger sudden drop for large *c/Ø* ratios and a smoother transition for small *c/Ø* ratios.

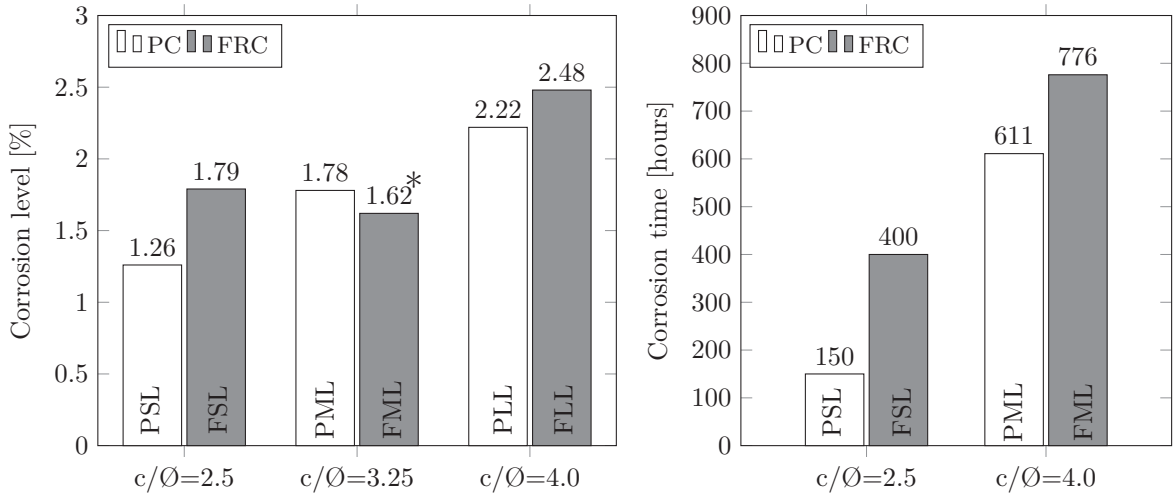

Figure 5: Crack initiation determined from corrosion level (a) and from corrosion time (b). *FML specimens yielded results in contradiction with the general trend shown by the remaining specimens.

It is also noteworthy that the initial range of electrical resistance in Fig. 3 and Fig. 4 showed no significant difference for plain and fibre reinforced concrete. This suggests that steel fibres were not conducting current under the applied DC field, hence the resistivity of FRC remained unchanged, a result that contradicts resistivity measurements carried out under AC [10].

A closer look to the embedded fibres, once the specimens had been split to extract the reinforcing bar, revealed that fibres were generally free of any signs of corrosion despite mixing 4% NaCl by weight of cement in the concrete and placing the specimens in 3.5% NaCl solution. This observation supports previous research indicating that steel fibres have higher resistance to chloride induced corrosion in concrete than steel reinforcement [11]. Nevertheless, some fibres located near the reinforcing bar presented evidences of light corrosion as shown in Fig. 6. Local defects, corrosion-induced cracks or a locally altered chloride-rich environment near the rebar promoted by ion migration under the applied DC field, might have been factors impairing the corrosion resistance of the observed corroded fibres.

Figure 6: Example of embedded fibres located near the rebar revealing light corrosion.

4. Conclusions

In this study experiments were carried out to determine the influence of adding 0.5% vol. steel fibres into concrete on initiation of corrosion-induced cracks in conventionally reinforced specimens. The results showed that fibres had a beneficial effect in terms of delayed crack initiation, which was more evident for small *c/Ø* ratios. This was attributed to a change in crack propagation from sudden for large cover, to gradual for small cover. Although fibres did not suppress cracking, it is argued that they would limit the crack width and prevent cover spalling at later stages. The experiments also revealed that steel fibres did not decrease the electrical resistivity of concrete based on the measured electrical resistance. The high corrosion resistance of steel fibres was confirmed by the lack of corrosion signs in the vast majority of embedded fibres.

References

[1] A. Poursaee and C. M. Hansson, "The influence of longitudinal cracks on the corrosion protection afforded reinforcing steel in high performance concrete," *Cem. Concr. Res.*, vol. 38, no. 8–9, pp. 1098–1105, Aug. 2008.

[2] H. Abrishami and D. Mitchell, "Influence of steel fibers on tension stiffening," *ACI Struct. J.*, vol. 94, pp. 769–776, 1997.

[3] F. Minelli, G. Tiberti, and G. A. Plizzari, "Durability and Crack control in FRC RC elements : an experimental study," in *International RILEM Conference on Advances in Construction Materials Through Science and Engineering*, 2011, pp. 435–443.

[4] G. Jen and C. P. Ostertag, "Resistance to Corrosion Induced Cracking in Self Consolidating Hybrid Fiber Reinforced Concrete," in *High Performance Fiber Reinforced Cement Composites 6*, vol. 2, 2012, pp. 163–170.

[5] R. H. Haddad and A. M. Ashteyate, "Role of synthetic fibers in delaying steel corrosion cracks and improving bond with concrete," *Can. J. Civ. Eng.*, vol. 28, no. 5, pp. 787–793, 2001.

[6] "EN 12390-3:2009 Testing hardened concrete. Part 3: Compressive strength of test specimens." 2009.

[7] "EN 12390-6:2001 Testing hardened concrete. Tensile splitting strength of test specimens." 2001.

[8] T. El Maaddawy and K. Soudki, "A model for prediction of time from corrosion initiation to corrosion cracking," *Cem. Concr. Compos.*, vol. 29, no. 3, pp. 168–175, 2007.

[9] ASTM G1, "Standard Practice for Preparing , Cleaning , and Evaluating Corrosion Test," 1999.

[10] C. G. Berrocal, K. Lundgren, and I. Löfgren, "Corrosion of steel bars embedded in fibre reinforced concrete under chloride attack: State of the art," *Cem. Concr. Res.*, vol. 80, pp. 69–85, Feb. 2016.

[11] P. S. Mangat and K. Gurusamy, "Corrosion Resistance of Steel Fibres in Concrete under Marine Exposure," *Cem. Concr. Res.*, vol. 18, pp. 44–54, 1988.